2D Hetero-nanostructures Hot Paper

DOI: 10.1002/anie.201410890

Liquid-Phase Epitaxial Growth of Two-Dimensional Semiconductor Hetero-nanostructures**

*Chaoliang Tan, Zhiyuan Zeng, Xiao Huang, Xianhong Rui, Xue-Jun Wu, Bing Li, Zhimin Luo, Junze Chen, Bo Chen, Qingyu Yan, and Hua Zhang**

Abstract: *Although many two-dimensional (2D) hybrid nanostructures are being prepared, the engineering of epitaxial 2D semiconductor hetero-nanostructures in the liquid phase still remains a challenge. The preparation of 2D semiconductor hetero-nanostructures by epitaxial growth of metal sulfide nanocrystals, including CuS, ZnS and Ni_3S_2, is achieved on ultrathin TiS_2 nanosheets by a simple electrochemical approach by using the TiS_2 crystal and metal foils. Ultrathin CuS nanoplates that are 50–120 nm in size and have a triangular/hexagonal shape are epitaxially grown on TiS_2 nanosheets with perfect epitaxial alignment. ZnS and Ni_3S_2 nanoplates can be also epitaxially grown on TiS_2 nanosheets. As a proof-of-concept application, the obtained 2D CuS–TiS_2 composite is used as the anode in a lithium ion battery, which exhibits a high capacity and excellent cycling stability.*

Engineering hetero-epitaxial nanostructures by depositing one kind of nanocrystals (for example, noble metals) on the other substrate with preferred orientation[1–3] have been demonstrated to be one of the most promising ways to achieve superior performances in a wide range of applications in plasmonics,[2a] catalysis,[2b,d,3b,d] electronics,[3a] and sensing.[3g] Gas-phase epitaxy methods are traditional techniques for epitaxial deposition of noble-metal nanostructures on bulk crystalline substrates.[2] However, they are limited by the low yield, high cost, and requirement of high temperature and ultra-high vacuum. In contrast, the liquid-phase epitaxy methods can overcome the aforementioned disadvantages. Until now, various epitaxial hetero-nanostructures, such as chalchogenide–chalchogenide,[3a] metal–metal,[3b–e] metal–metal oxide,[3f,g] and metal–chalchogenide,[3h] have been prepared by solution-based synthetic methods, and they presented greatly enhanced performance in electrocatalysis,[3b,d] sensing,[3g] and electronics,[3a] which is due to their well-defined structures, interfaces, and selectively-exposed facets. However, all the aforementioned epitaxial hybrid nanomaterials are based on the formation of core–shell nanoparticles or nanoparticle-based hybrid nanomaterials. Therefore, the epitaxial growth of anisotropic nanocrystals, and especially two-dimensional (2D) nanostructures, on dispersible templates still remains challenge.

Recently, single- or few-layer transition-metal dichalcogenide (TMD) nanosheets,[4] such as MoS_2, TiS_2, TaS_2, WS_2, have been emerging as a newly unique class of 2D nanomaterials and have shown many promising applications in electronics,[4e,f] catalysis,[4g] sensing,[4h] and energy storage,[4i] owing to their outstanding physical, electronic, and electrochemical properties. These TMD nanosheets can be used as novel templates for the construction of functional composites or directing the growth/assembly of some unique nanostructures.[5] As a typical example, our group first demonstrated the epitaxial growth of noble metal nanocrystals including Pt, Pd, and Ag on single-layer MoS_2 nanosheets in solution under ambient conditions.[5a] Although 2D lateral or vertical epitaxial TMD hetero-nanostructures, such as MoS_2-$MoSe_2$, WS_2-WSe_2, $MoSe_2$-WSe_2, and WS_2-MoS_2, have been achieved by using chemical vapor deposition methods very recently,[6] the liquid-phase growth of 2D TMD epitaxial hetero-nanostructures still remains a challenge. Herein, for the first time, we report a facile and universal method for the liquid-phase epitaxial growth of metal sulfide nanoplates including CuS, ZnS, and Ni_3S_2 on the ultrathin TiS_2 nanosheets to obtain a new type of 2D vertical epitaxial hetero-nanostructures, referred to as CuS–TiS_2, ZnS–TiS_2, and Ni_3S_2–TiS_2, respectively. It is worth pointing out that the CuS nanoplates with a size of 50–120 nm and triangular or hexagonal shape were deposited on TiS_2 nanosheets with perfect epitaxial alignment without any misorientation. As a proof-of-concept application, the obtained 2D CuS–TiS_2

[*] C. L. Tan,[+] Dr. Z. Y. Zeng,[+] Dr. X. Huang,[+] Dr. X. H. Rui, Dr. X.-J. Wu, Dr. Z. M. Luo, J. Z. Chen, B. Chen, Prof. Q. Y. Yan, Prof. H. Zhang
School of Materials Science and Engineering
Nanyang Technological University
50 Nanyang Avenue, Singapore 639798 (Singapore)
E-mail: hzhang@ntu.edu.sg
Homepage: http://www.ntu.edu.sg/home/hzhang/

Dr. X. Huang[+]
Key Laboratory of Flexible Electronics (KLOFE) and Institute of Advanced Materials (IAM), National Jiangsu Synergistic Innovation Center for Advanced Materials (SICAM)
Nanjing Tech University (NanjingTech)
30 South Puzhu Road, Nanjing 211816 (China)

Dr. B. Li
Institute of Materials Research and Engineering
A*STAR (Agency for Science, Technology and Research)
3 Research Link, Singapore 117602 (Singapore)

[+] These authors contributed equally to this work.

[**] This work was supported by the MOE under AcRF Tier 2 (ARC 26/13, No. MOE2013-T2-1-034), AcRF Tier 1 (RG 61/1, RGT18/13, and RG5/13), a Start-Up Grant (M4080865.070.706022), the Singapore Millennium Foundation, and the National Research Foundation in Singapore. This research is also conducted by NTU-HUJ-BGU Nanomaterials for Energy and Water Management Programme under the Campus for Research Excellence and Technological Enterprise (CREATE), that is supported by the National Research Foundation, Prime Minister's Office, Singapore.

Supporting information for this article is available on the WWW under http://dx.doi.org/10.1002/anie.201410890.

hetero-nanostructure was used as an anode of a Li-ion battery, which exhibited a large capacity and excellent cycling performance.

The preparation of 2D semiconductor epitaxial hetero-nanostructures, that is, CuS–TiS_2, ZnS–TiS_2, and Ni_3S_2–TiS_2, is described in the experimental section in detail (see the Supporting Information). Briefly, the TiS_2 crystal powder was first mixed with acetylene black and poly(vinylidene fluoride) (PVDF) in N-methylpyrrolidone (NMP) to from a homogeneous slurry, which was then coated on metal foil (for example, Cu, Zn, or Ni), and assembled in a Li-ion battery cell as cathode. After Li ions were intercalated into the layered TiS_2 crystals during the discharge process, the battery cell was kept undisturbed for about two weeks. Finally, the TiS_2-coated electrode was taken out from the battery cell and washed with acetone, followed by sonication in water. The resultant solution was then centrifuged to obtain the final product, that is, CuS–TiS_2, ZnS–TiS_2, or Ni_3S_2–TiS_2, which are characterized as follows.

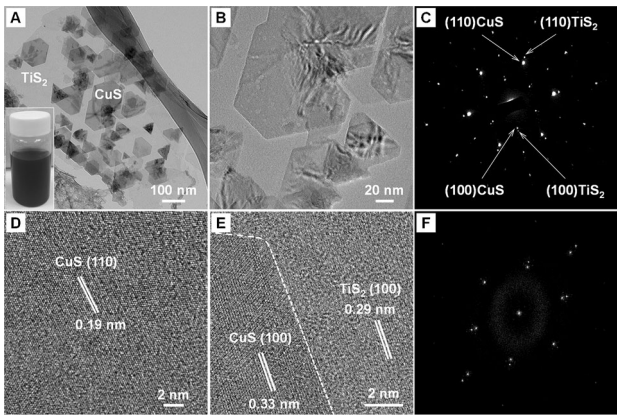

Figure 1. TEM analysis of CuS–TiS_2 hetero-nanostructures. A) TEM image of CuS nanoplates epitaxially grown on a TiS_2 nanosheet. Inset: photograph of CuS–TiS_2 solution. B) Highly magnified TEM image of CuS–TiS_2. C) The SAED pattern of CuS–TiS_2 with the electron beam perpendicular to the basal plane of TiS_2 nanosheet. D) HRTEM image of a typical CuS nanoplate on TiS_2 nanosheet. E) HRTEM image and F) its corresponding FFT-generated SAED pattern of a typical CuS nanoplate on TiS_2 nanosheet. The dotted curve in (E) roughly shows the interface between CuS and TiS_2.

The transmission electron microscopy (TEM) was used to characterize the CuS–TiS_2 hetero-nanostructure. As shown in Figure 1 A,B, it can be observed that small CuS nanoplates with size of 50–120 nm in triangular or hexagonal shape were grown on the TiS_2 nanosheet. The selected area electron diffraction (SAED) pattern of CuS–TiS_2 showed two sets of diffraction spots with six-fold symmetry, which can be indexed to CuS and TiS_2, respectively (Figure 1 C). The six spots of (110) planes of CuS with a lattice spacing of 0.19 nm are perfectly aligned to the six spots of (110) planes of TiS_2 with a lattice spacing of 0.17 nm. Another six spots of CuS, which correspond to (100) planes with a lattice spacing of 0.33 nm, are well aligned with the six spots of TiS_2(100) planes with a lattice spacing of 0.29 nm. These well-aligned SAED patterns between CuS and TiS_2 clearly demonstrated that the CuS nanoplates were epitaxially grown on TiS_2 sheets. Importantly, there is no any misorientation observed in the epitaxial growth of CuS on TiS_2 nanosheet. The high-resolution TEM (HRTEM) image of a typical CuS nanoplate confirmed its single-crystalline structure. The measured lattice distance is about 0.19 nm (Figure 1 D), which is assignable to the (110) planes of hexagonal CuS and can be indexed to the hexagonal phase covellite in the space group of $P6_3/mmc$ (JCPDS 06-0464 with $a = 3.792$ Å and $c = 16.340$ Å). The HRTEM image at the interface of CuS and TiS_2 clearly showed their lattice fringes (Figure 1 E). As shown in Figure 1 F, two sets of well-aligned spots, which are very similar to the SAED patterns in Figure 1 C, can be observed from the fast Fourier transfer (FFT)-generated SAED pattern originated from Figure 1 E, further confirming the epitaxial growth of CuS nanoplates on TiS_2 sheet.

Figure 2 A illustrates the CuS–TiS_2 hetero-nanostructure. The epitaxial relationship between the CuS nanoplate and TiS_2 substrate was shown in Figure 2 B. It can be seen that the sulfur layers in CuS and TiS_2 exhibit the same hexagonal symmetry, with a lattice mismatch of about 10 % given that the *d*-spacings for CuS (110) and TiS_2 (110) are 0.19 and 0.17 nm, respectively. Interestingly, the TEM image also showed the Moiré pattern fringes that were produced by the presence of two superimposed lattice planes with different lattice spacings, that is, CuS and TiS_2 in this work (Supporting Information, Figure S1).[7] The measured Moiré pattern spacing is about 1.52 nm, which is close to the calculated value (1.615 nm) of the Moiré pattern spacing, which corresponds to the superimposed (110) planes of epitaxially stacked CuS and TiS_2, based on the reported calculation method.[8]

Moreover, the energy-dispersive X-ray spectroscopy (EDS) and corresponding elemental mapping were used to explore the composition of the CuS–TiS_2 hetero-nanostructures. The presence of S, Ti, and Cu, and their homogeneous

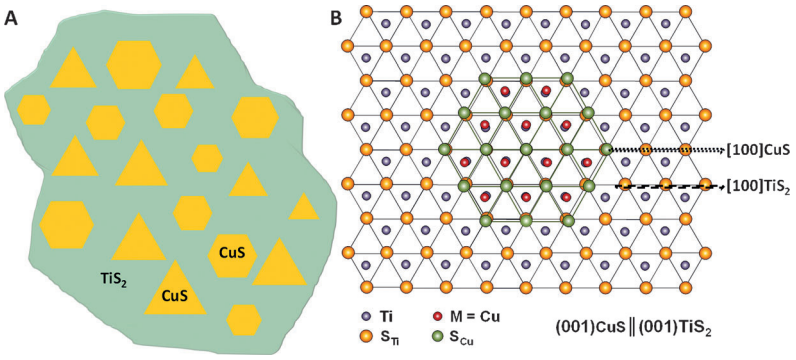

Figure 2. Representation of the epitaxial growth of CuS nanoplates on TiS_2 nanosheets. A) Illustration showing CuS nanoplates epitaxially grown on a TiS_2 naosheet. B) Azimuthal orientation of a CuS nanoplate on the TiS_2(001) surface in the (001) orientation. Only the top S and Ti layer of TiS_2 and bottom S and Cu layer of CuS are shown.

distribution in the hetero-nanostructures, can be clearly observed in the Supporting Information, Figure S2A–D. The corresponding EDS spectrum showed strong signals of S, Ti and Cu elements (Supporting Information, Figure S2E). The ratio of CuS to TiS_2 is about 3:2, which was calculated from the EDS result (Supporting Information, Table S1). Note that the weak O signal observed in the EDS spectrum (Supporting Information, Figure S2E) may arise from oxidation of the sample prior to the characterization. Furthermore, the chemical composition of CuS–TiS_2 was investigated by X-ray photoelectron spectroscopy (XPS). The XPS survey spectrum of CuS–TiS_2 showed the obvious signals of Cu, Ti, S, and O (Supporting Information, Figure S3A). As shown in Figure S3B, the fitted Cu spectrum exhibited two peaks at 931.5 and 951.5 eV, indicating that Cu^{2+} in CuS is the main signal.[9a] The Ti^{4+} in TiS_2 was detected as the dominant oxidation state, as shown in the fitted Ti spectrum (Supporting Information, Figure S3C).[9b,c] The S^{2-} in CuS and TiS_2 was fitted as the dominant state of S spectrum (Supporting Information, Figure S3D).[9]

To investigate the growth process of CuS–TiS_2, the products at different reaction times were characterized by TEM. In our experiment, after Li ions were intercalated into TiS_2 on the Cu electrode during the discharge process, the battery cell was kept undisturbed for a certain time before the electrode was taken out. The reaction time here means the undisturbed time in which the reaction continuously happens. Figure 3 shows the TEM images and corresponding SAED patterns of the products obtained at different reaction time. At 1 day, pure TiS_2 nanosheets were obtained (Figure 3 A,B), which is consistent with our previous report.[10] Notably, some small CuS nanocrystals can be observed on TiS_2 sheets at reaction time of 5 days (Figure 3 C). The corresponding SAED pattern showed that the CuS nanocrystals were epitaxially deposited on TiS_2 (Figure 3 D). The CuS nanocrystals continuously grew to form CuS nanoplates with a triangular shape at reaction time of 10 days, which were aligned on TiS_2 sheets (Figure 3 E). The epitaxial growth is clearly evidenced by the corresponding SAED pattern (Figure 3 F). After the electrode was kept undisturbed for 15 days, some relatively large CuS nanoplates with triangular or hexagonal shapes were obtained on TiS_2 sheets with perfect epitaxial alignment (Figure 3 G,H).

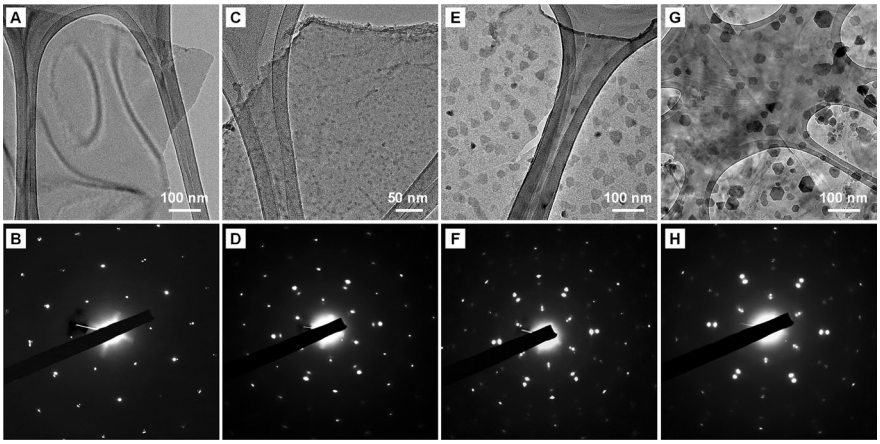

Figure 3. TEM images and the corresponding SAED patterns of products obtained at different time: A,B) 1 d, C,D) 5 d, E,F) 10 d, and G,H) 15 d.

Significantly, our method is widely applicable for epitaxial growth of other metal sulfide on TiS_2 sheets. By replacing the Cu foil with Zn or Ni foil, ZnS or Ni_3S_2 nanoplates can be also epitaxially deposited on TiS_2 nanosheets at the similar experimental conditions. As shown in the Supporting Information, Figure S4A, ZnS nanoplates with size of 70–150 nm grown on TiS_2 nanosheets can be observed. Its corresponding SAED pattern revealed the epitaxial growth effect of ZnS on TiS_2 (Supporting Information, Figure S4B). The HRTEM image at the interface of ZnS–TiS_2 showed two crystalline structures with lattice fringes of 0.29 and 0.27 nm, which is assignable to both (100) planes of TiS_2 and ZnS (Supporting Information, Figure S4C). The EDX spectrum of ZnS–TiS_2 hetero-nanostructures clearly showed the presence of Zn, Ti, and S (Supporting Information, Figure S5). Similarly, Ni_3S_2 nanoplates with a size of 50–200 nm can be also epitaxially grown on TiS_2 nanosheets, and the detail TEM and EDS analyses are shown in the Supporting Information, Figure S4D,F and Figure S6, respectively.

In our experiment, the bulk TiS_2 crystals and metal foils were used as the starting materials. Previously, our group used the lithium intercalation method for exfoliation of single-layer 2D TMD nanosheets from their bulk crystals.[10] Taking TiS_2 as an example, after the discharging process, the Li ions were intercalated into the interlayer spacing of TiS_2 crystal and reacted with TiS_2 to form the intercalated compound, that is, Li_xTiS_2.[10] It has been reported that during the lithium intercalation process, Li can react with TiS_2 to form Li_2S through the following reactions:[11]

$$Li + TiS_2 \rightarrow {}^1/_2\,Ti_2S_3 + {}^1/_2\,Li_2S \quad (1);$$

$$Li + {}^1/_2\,TiS_2 \rightarrow {}^1/_2\,TiS + {}^1/_2\,Li_2S \quad (2);$$

and $$Li + {}^1/_4\,TiS_2 \rightarrow {}^1/_4\,Ti + {}^1/_2\,Li_2S \quad (3).$$

According to the previous study, by coating S powder on Cu foil as the anode in a battery cell, CuS nanocrystals were obtained after the discharging process.[12] In their experiment, the S powder reacted with Li to form Li_2S and the Li_2S then reacted with Cu foil to obtain the CuS nanocrystals. Therefore, in our experiment, we suggest that during the electrochemical process, Li first reacted with TiS_2 crystal to form the Li_xTiS_2 compound, in which the interlayer spacing of TiS_2 crystal was expanded. Meanwhile, some Li_2S could also be obtained based on the reaction between Li and TiS_2 [Eq. (1)–(3)]. The formed Li_2S then reacted with Cu foil to get CuS nanocrystals. Because of the similar crystal symmetry of CuS and TiS_2 nanosheet and tolerable lattice mismatch (ca. 10%), the epitaxial growth of CuS on TiS_2 was realized to minimize the free energy at their interface. The mechanism for growth of ZnS and Ni_3S_2 on TiS_2 sheets are similar to the aforementioned mechanism for CuS–TiS_2.

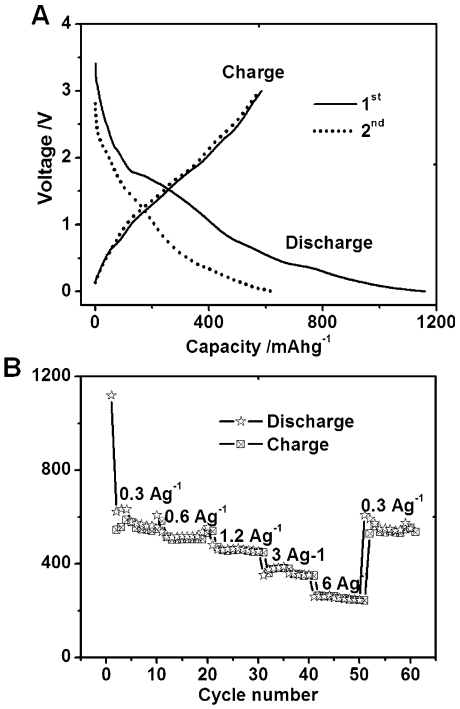

Figure 4. Lithium ion battery performance of the CuS–TiS_2 hetero-nanostructure. A) Charge–discharge voltage profile of the CuS–TiS_2 electrode at current density of 0.3 $A g^{-1}$ for the first two cycles. B) Cycling performance of the CuS–TiS_2 electrode at various current densities.

As a proof-of-concept application, the CuS–TiS_2 hetero-nanostructure was used as anode in Li-ion battery. The first two charge–discharge curves at current density of 0.3 $A g^{-1}$ are shown in Figure 4 A. The first intercalation process gave discharge capacity of 1158 $mAh g^{-1}$ and a corresponding charge capacity of 584 $mAh g^{-1}$, which means the first Coulombic efficiency is only 50.4 %, along with solid electrolyte interphase formation, the initial irreversible capacity may also attribute to the incomplete de-intercalation of Li ions that intercalated into CuS–TiS_2. During the second cycle, the electrode showed discharge capacity of 626 $mAh g^{-1}$ with charge capacity of 578 $mAh g^{-1}$. It is worth pointing out that the capacity of CuS–TiS_2 hetero-nanostructure is higher than that of the pure CuS nanosheet and TiS_2 based batteries.[13] Importantly, the fabricated battery cell shows excellent cycling performance. As shown in the Supporting Information, Figure S7, the specific capacity of CuS–TiS_2 based battery almost keeps same even after 100 cycles (ca. 600 $mAh g^{-1}$). The high reversible capacity and excellent cycling behavior of CuS–TiS_2 is also demonstrated in the rate capability. The cycling performance of CuS–TiS_2 composite at different current densities is shown in Figure 4 B. It was found that the CuS–TiS_2 battery exhibits capacities as high as about 350 and about 260 $mAh g^{-1}$ at high current densities of 3 and 6 $A g^{-1}$, respectively (Figure 4 B). This performance is much better than that of pure CuS nanosheets.[13a] Importantly, even after the charging–discharging process at high current density, the capacity of CuS–TiS_2 battery can be fully recovered to the initially stable value (Figure 4 B). The large specific capacity and excellent cycling performance make CuS–TiS_2 a promising material for Li ion battery application.

In summary, we have developed a facile and general method for the preparation of vertical 2D epitaxial semiconductor hetero-nanostructures, including CuS–TiS_2, ZnS–TiS_2, and Ni_3S_2–TiS_2. Thin CuS nanoplates with triangular/hexagonal shape were epitaxially grown on TiS_2 nanosheets with perfect epitaxial alignment without any misorientation. To the best of our knowledge, this is the first time that the epitaxial growth of 2D semiconductor hetero-nanostructures was achieved in the liquid phase at room temperature. Intriguingly, the obtained 2D CuS–TiS_2 hetero-nanostructure was used as anode in lithium-ion battery, which exhibited a large capacity and excellent cycling stability. We believe that our facile and universal method could be a promising strategy towards the scalable production of novel 2D hybrid nanomaterials with well-defined structures for various applications.

Received: November 10, 2014
Published online: December 21, 2014

Keywords: CuS nanoplates · epitaxial growth · hetero-nanostructures · TiS_2 nanosheets

[1] R. Costi, A. E. Saunders, U. Banin, *Angew. Chem. Int. Ed.* **2010**, *49*, 4878 – 4897; *Angew. Chem.* **2010**, *122*, 4996 – 5016.
[2] a) P. Nagpal, N. C. Lindquist, S. H. Oh, D. J. Norris, *Science* **2009**, *325*, 594 – 597; b) V. Komanicky, H. Iddir, K. C. Chang, A. Menzel, G. Karapetrov, D. Hennessy, P. Zapol, H. You, *J. Am. Chem. Soc.* **2009**, *131*, 5732 – 5733; c) Y. Yoo, K. Seo, S. Han, K. S. K. Varadwaj, H. Y. Kim, J. H. Ryu, H. M. Lee, J. P. Ahn, H. Ihee, B. Kim, *Nano Lett.* **2010**, *10*, 432 – 438; d) J. A. Enterkin, K. R. Poeppelmeier, L. D. Marks, *Nano Lett.* **2011**, *11*, 993 – 997.
[3] a) X. G. Peng, M. C. Schlamp, A. V. Kadavanich, A. P. Alivisatos, *J. Am. Chem. Soc.* **1997**, *119*, 7019 – 7029; b) S. E. Habas, H. Lee, V. Radmilovic, G. A. Somorjai, P. D. Yang, *Nat. Mater.* **2007**, *6*, 692 – 697; c) C. Xue, J. E. Millstone, S. Li, C. A. Mirkin, *Angew. Chem. Int. Ed.* **2007**, *46*, 8436 – 8439; *Angew. Chem.* **2007**, *119*, 8588 – 8591; d) C. L. Lu, K. S. Prasad, H. L. Wu, J. A. A. Ho, M. H. Huang, *J. Am. Chem. Soc.* **2010**, *132*, 14546 – 14553; e) D. Seo, C. I. Yoo, J. Jung, H. Song, *J. Am. Chem. Soc.* **2008**, *130*, 2940 – 2941; f) F. Ru Fan, Y. Ding, D. Y. Liu, Z. Q. Tian, Z. L. Wang, *J. Am. Chem. Soc.* **2009**, *131*, 12036 – 12037; g) X. L. Sun, S. J. Guo, Y. Liu, S. H. Sun, *Nano Lett.* **2012**, *12*, 4859 – 4863; h) W. S. Wang, J. Goebl, L. He, S. Aloni, Y. X. Hu, L. Zhen, Y. D. Yin, *J. Am. Chem. Soc.* **2010**, *132*, 17316 – 17324.
[4] a) M. Chhowalla, H. S. Shin, G. Eda, L. J. Li, K. Loh, H. Zhang, *Nat. Chem.* **2013**, *5*, 263 – 275; b) V. Nicolosi, M. Chhowalla, M. G. Kanatzidis, M. S. Strano, J. N. Coleman, *Science* **2013**, *340*, 1226419; c) X. Huang, Z. Y. Zeng, H. Zhang, *Chem. Soc. Rev.* **2013**, *42*, 1934 – 1946; d) H. S. S. Ramakrishna Matte, A. Gomathi, A. K. Manna, D. J. Late, R. Datta, S. K. Pati, C. N. R. Rao, *Angew. Chem. Int. Ed.* **2010**, *49*, 4059 – 4062; *Angew. Chem.* **2010**, *122*, 4153 – 4156; e) B. Radisavljevic, A. Radenovic, J. Brivio, V. Giacometti, A. Kis, *Nat. Nanotechnol.* **2011**, *6*, 147 – 150; f) C. W. Lin, X. J. Zhu, J. Feng, C. Z. Wu, S. L. Hu, J. Peng, Y. Q. Guo, L. L. Peng, J. Y. Zhao, J. L. Huang, J. L. Yang, Y. Xie, *J. Am. Chem. Soc.* **2013**, *135*, 5144 – 5151; g) D. Voiry, H. Yamaguchi, J. W. Li, R. Silva, D. C. B. Alves, T. Fujita, M. W. Chen, T. Asefa, V. B. Shenoy, G. Eda, M. Chhowalla, *Nat. Mater.* **2013**, *12*, 850 – 855; h) C. F. Zhu, Z. Y. Zeng, H. Li, F. Li, C. H. Fan, H. Zhang, *J. Am. Chem. Soc.* **2013**, *135*, 5998 – 6001; i) G. D.

Du, Z. P. Guo, S. Q. Wang, R. Zeng, Z. X. Chen, H. K. Liu, *Chem. Commun.* **2010**, *46*, 1106 – 1108.
[5] a) X. Huang, Z. Y. Zeng, S. Y. Bao, M. F. Wang, X. Y. Qi, Z. X. Fan, H. Zhang, *Nat. Commun.* **2013**, *4*, 1444; b) C. L. Tan, X. Y. Qi, X. Huang, J. Yang, B. Zheng, Z. F. An, R. F. Chen, J. Wei, B. Z. Tang, W. Huang, H. Zhang, *Adv. Mater.* **2014**, *26*, 1735 – 1739; c) C. L. Tan, H. Zhang, *Chem. Soc. Rev.* **2015**, DOI: 10.1039/c4s00182f; d) X. Huang, C. L. Tan, Z. Y. Yin, H. Zhang, *Adv. Mater.* **2014**, *26*, 2185 – 2204.
[6] a) X. D. Duan, C. Wang, J. C. Shaw, R. Cheng, Y. Chen, H. H. Li, X. P. Wu, Y. Tang, Q. L. Zhang, A. L. Pan, J. H. Jiang, R. Q. Yu, Y. Huang, X. F. Duan, *Nat. Nanotechnol.* **2014**, *9*, 1024 – 1030; b) C. M. Huang, S. F. Wu, A. M. Sanchez, J. J. P. Peters, R. Beanland, J. S. Ross, P. Rivera, W. Yao, D. H. Cobden, X. D. Xu, *Nat. Mater.* **2014**, *13*, 1096 – 1101; c) Y. J. Gong, J. H. Lin, X. L. Wang, G. Shi, S. D. Lei, Z. Lin, X. L. Zou, G. L. Ye, R. Vajtai, B. I. Yakobson, H. Terrones, M. Terrones, B. K. Tay, J. Lou, S. T. Pantelides, Z. Liu, W. Zhou, P. M. Ajayan, *Nat. Mater.* **2014**, *13*, 1135 – 1142.
[7] M. Grzelczak, B. Rodríguez-González, J. Pérez-Juste, L. M. Liz-Marzán, *Adv. Mater.* **2007**, *19*, 2262 – 2266.
[8] F. R. Fan, D. Y. Liu, Y. F. Wu, S. Duan, Z. X. Xie, Z. Y. Jiang, Z. Q. Tian, *J. Am. Chem. Soc.* **2008**, *130*, 6949 – 6951.
[9] a) E. Z. Kurmaevy, J. van Ek, D. L. Ederer, L. Zhou, T. A. Callcott, R. C. C. Perera, V. M. Cherkashenko, S. N. Shamin, V. A. Trofimova, S. Bartkowski, M. Neumann, A. Fujimori, V. P. Moloshag, *J. Phys. Condens. Matter* **1998**, *10*, 1687 – 1697; b) M. G. Faba, D. Gonbeau, G. Pfister-guillouzo, *J. Electron. Spectrosc.* **1995**, *73*, 65 – 80; c) J. C. Dupin, D. Gonbeau, I. Martin-Litas, P. Vinatier, A. Levasseur, *Appl. Surf. Sci.* **2001**, *173*, 140 – 150.
[10] a) Z. Y. Zeng, Z. Y. Yin, X. Huang, H. Li, Q. Y. He, G. Lu, F. Boey, H. Zhang, *Angew. Chem. Int. Ed.* **2011**, *50*, 11093 – 11097; *Angew. Chem.* **2011**, *123*, 11289 – 11293; b) Z. Y. Zeng, C. L. Tan, X. Huang, S. Y. Bao, H. Zhang, *Energy Environ. Sci.* **2014**, *7*, 797 – 803.
[11] a) M. S. Whittingham, *J. Electrochem. Soc.* **1976**, *123*, 315 – 320; b) D. W. Murphy, J. N. Carides, *J. Electrochem. Soc.* **1979**, *126*, 349 – 351.
[12] Y. R. Wang, X. W. Zhang, P. Chen, H. T. Liao, S. Q. Cheng, *Electrochim. Acta* **2012**, *80*, 264 – 268.
[13] a) Y. P. Du, Z. Y. Yin, J. X. Zhu, X. Huang, X. J. Wu, Z. Y. Zeng, Q. Y. Yan, H. Zhang, *Nat. Commun.* **2012**, *3*, 1177; b) G. L. Che, K. B. Jirage, E. R. Fisher, C. R. Martin, H. Yoneyama, *J. Electrochem. Soc.* **1997**, *144*, 4296 – 4302.

